Biochemical Pharmacology, Vol. 55, pp. 1475–1479, 1998.

ISSN 0006-2952/98/$19.00 + 0.00
S0006-2952(97)00659-X

Cellular Distribution of *N*-Acetyltransferase Activity in the Rat Small Intestine

Joseph A. Ware, Timothy P. Reilly and Craig K. Svensson†*
Department of Pharmaceutical Sciences, Wayne State University, Detroit, MI 48202, U.S.A.

ABSTRACT. The cellular distribution of AcCoA:arylamine *N*-acetyltransferase (NAT; EC 2.3.1.5) activities was examined in the rat small intestine to determine if heterogeneous cellular distribution contributes to preferential tumor development in the colonic region after exposure to heterocyclic amines (HAs). A chelation/elution method was used to preferentially isolate villus-tip, mid-villus, and crypt enterocytes. Monomorphic (NAT1) and polymorphic (NAT2) activities were determined using *N*-acetylprocainamide and *N*-acetamidobenzoic acid formation, respectively. Sucrase-isomaltase (SI) activity was used to confirm that a villus, mid-villus, and crypt cell gradient had been obtained. Utilizing this marker of villus enrichment, a 4- to 10-fold gradient was achieved. NAT1 and NAT2 activities followed this gradient, with the highest NAT activity occurring in the fraction with the highest SI activity. The ratio of NAT2:NAT1 remained essentially constant along the gradient, indicating a similar pattern of expression for both enzymes. This pattern of cellular distribution for the NATs is similar to that reported for cytochrome P450s. This apparent preferential expression of NAT in the villus cells may result in delivery of bioactivated HAs to the lower regions of the intestines as the villus-tip cells are extruded into the intestinal lumen and enter the fecal stream. BIOCHEM PHARMACOL **55**;9: 1475–1479, 1998. © 1998 Elsevier Science Inc.

KEY WORDS. acetyltransferases; intestinal metabolism; enterocytes; N-acetylation; heterocyclic amines

The gastrointestinal mucosa represents the first biological barrier encountered by orally ingested xenobiotics. This barrier includes a variety of cells, some of which contain enzymes capable of catalyzing the biotransformation of xenobiotics to toxic or non-toxic metabolites. Several studies have shown that a wide array of xenobiotic-metabolizing enzymes (including CYP,‡ sulfotransferases and NATs) are present in the gastrointestinal tract of both humans and animals [1, 2].

As many xenobiotic-induced toxicities are believed to result from the formation of reactive metabolites [3, 4], there is significant interest in determining the ability of target tissues to catalyze the biotransformation of xenobiotics. For example, it is known that ingestion of HAs results in colorectal tumor formation in the F-344 rat [5]. This regiospecific tumor formation may result from heterogeneous distribution of bioactivating enzymes, such that the region of greatest susceptibility is also that which exhibits the highest rate of bioactivation. One enzyme family believed to play an important role in the bioactivation of HAs is the NATs.

Recently, we reported that the distribution of NAT1 and NAT2 did not differ along the length of the small and large intestine of the F-344 rat [6]. Thus, preferential biotransformation in the colonic region does not appear to explain the propensity for tumor development in the lower regions of the gastrointestinal tract. While relatively homogeneous longitudinal distribution of these enzymes was observed, it is important to recognize that cell turnover in these intestinal regions differs markedly. The epithelium of the small intestine undergoes continuous cellular proliferation within the crypts and differentiation at the crypt-villus junction, prior to cell extrusion into the gut lumen [7–10]. Vertical heterogeneity, where there is preferential expression of NAT in the crypt or villus regions, could markedly influence the role of the bioactivation of HAs in the small intestine. If enzymes are preferentially expressed in the villus-tip, recently extruded cells may selectively deliver bioactivated HA to the lower regions of the intestine. In contrast, preferential distribution of the enzymes in the crypt cells may result in cellular transformations that alter the normal proliferation and/or differentiation and movement along the crypt-villus axis.

While other investigators have established the vertical heterogeneity and regulation of CYP enzymes [11–16], little is known about the vertical distribution of the phase II xenobiotic-metabolizing enzymes [17], in particular, the

*Present address: Molecular and Cellular Toxicology Section, Laboratory of Molecular Immunology, National Institutes of Health, Bldg. 10, Rm. 8N110, Bethesda, MD 20892-1760.

† Corresponding author: Tel. (313) 577-0823; FAX (313) 577-0233; E-mail: cks@wizard.pharm.wayne.edu.

‡ *Abbreviations:* CYP, cytochrome P450; DTT, dithiothreitol; GST, glutathione *S*-transferase; HAs, heterocyclic amines; NAPA, *N*-acetylprocainamide; NAPABA, *N*-acetylPABA; NAT, *N*-acetyltransferase; PA, procainamide; PABA, *p*-aminobenzoic acid; PGO, peroxidase-glucose oxidase; PMSF, phenylmethylsulfonyl fluoride; RMANOVA, repeated measures analysis of variance; SI, sucrase-isomaltase; and SNK, Student–Newman–Keuls.

Received 10 July 1997; accepted 31 October 1997.

TABLE 1. Chelation/elution buffers for enterocyte isolation

Solution A		Solution B	
KCl	1.5 mM	PBS	
NaCl	96 mM	EDTA	1.5 mM
Sodium citrate	27 mM	DTT	0.5 mM
KH_2PO_4	8 mM	PMSF	40 μg/mL
Na_2HPO_4	5.6 mM	BSA	1 mg/mL
PMSF	40 μg/mL		
BSA	1 mg/mL		
DTT	1 mM		

NATs. The capacity to acetylate xenobiotics across the crypt-villus axis has, to our knowledge, not been reported. Therefore, we have examined the cellular distribution of NAT1 and NAT2 in the small intestine of the F-344 rat along the crypt to villus axis.

MATERIALS AND METHODS

Chemicals

Acetyl coenzyme A, DTT, BSA, PA, PABA, NAPABA, stock reagents, Triton X-100, Trizma base, and a Glucose Oxidase kit (PGO capsules that contain 500 units of glucose oxidase and 100 purpurogallin units of peroxidase, *o*-dianisidine dihydrochloride, glucose standard) were obtained from the Sigma Chemical Co. NAPA was a gift of E.R. Squibb & Sons, Inc. Date-of-birth matched male F-344 rats (175–200 g) were obtained from Charles River and were acclimated in a 12-hr light/dark cycle, humidity- and temperature-controlled environment for at least 72 hr before experimentation. Animals had access to standard rodent chow and water *ad lib*. All animals were killed between 7:30 and 9:30 a.m. on study days.

Animals and Enterocyte Isolation Protocol

On the day of enterocyte harvest, rats were killed by CO_2 inhalation, and a 30-cm segment of small intestine was removed starting 10 cm distal to the pyloric sphincter. An adaption of the chelation/elution method of Weiser [18] was used for isolation of enterocytes [14, 15], with elution solutions shown in Table 1. Briefly, after gently flushing ingesta and incubating the lumen with solution A for 15 min, the proximal lumen was cannulated intermittently using a stainless steel oral cannula connected to a 60-mL syringe for instillation of solution B. Hemostats were placed at the proximal and distal ends of the lumen for retention of the chelating solution. After the lumen was filled with solution B, the intestinal segment was placed in a 5 × 5 in. Rubbermaid® tray containing PBS with 20% (v/v) glycerol, and was maintained at 37° in a Dubnoff metabolic shaker bath during the isolation process. Enterocytes were eluted by release of the distal hemostat with collection of elution fractions into a conical polystyrene centrifuge tube. Once fractions were collected, all subsequent procedures were conducted at 4°. Input buffer volumes were recorded along with eluent (output) suspension volumes, and, in all experiments, greater than 85% recovery was attained.

Cellular Localization of NAT within the Small Intestine

Immediately after cell isolation, the cell suspension was washed with solution B followed by a 5-min low-speed centrifugation (35 *g*). Cellular fractions were combined from each animal (**1**, 2 + **3**, 4 + **5**, 6 + **7**, 8 + **9**, 10 + **11**, 12 + **13**, where bold represents subsequent fraction identification number) and suspended in Sorensen's phosphate buffer containing the protease inhibitors PMSF (50 μM) and leupeptin (10 μM), BSA (1 mg/mL), DTT (1 mM), and EDTA (1 mM). An aliquot of the cell suspension was removed for cell counting and viability testing via trypan blue dye exclusion. The remaining suspension was homogenized in a glass/teflon (Potter/Elvehjem) tissue homogenizer for 15 up/down strokes, followed by pulse sonication and differential centrifugation for subcellular fractionation. The 100,000 *g* supernatant of the pooled cellular fractions was utilized as the cytosolic source. NAT activity was determined as previously described for NAT1 (NAPA formation) and NAT2 (NAPABA formation), normalized per 10^6 cells or per milligram of cytosolic protein [19, 20].

Biochemical Marker of Enterocytic Cell Differentiation

A reliable biochemical marker of enterocyte differentiation is the expression of brush-border intestinal disaccharidase activity [18, 21]. SI is expressed only in differentiated crypt-villus and villus-tip enterocytes and is known to be regulated at the level of mRNA abundance [22, 23]. The assay for SI utilized in this series of experiments was modified from that originally described by Dahlqvist [24]. This assay quantifies sucrose hydrolysis (disaccharidase activity) to glucose, using purified glucose oxidase reagent and chromogen. Briefly, in a foil-covered flask under constant vacuum, the Tris glucose oxidase (TGO) reagent was prepared by adding 0.24 mL of Triton X-100 to 100 mL of degassed Tris buffer (0.5 M), pH adjusted to 7.0. Then one PGO capsule was emptied into the flask, followed by 4 mg *o*-dianisidine. This reagent was then transferred to an Optifix® dispenser and placed on ice until used. Homogenates were diluted 1:10 with PBS, and 100 μL of this suspension was added to a plastic spectrophotometric cuvette that contained 100 μL of 0.056 M of sucrose or buffer. These cuvettes were incubated at 37° in a covered shaker bath for 60 min, followed by the addition of 3 mL of TGO. After a 20-min incubation, a brilliant orange color developed, and absorbance was recorded at 452 nm. The amount of glucose formed was determined from a standard curve prepared from glucose standards and normalized per 10^6 cells. Preliminary studies indicated that glucose formation is linear with respect to time, concentration, and amount of protein present. [*Note: Because o-dianisidine (chromogen of Dahlqvist method) is considered mutagenic and carcinogenic,*

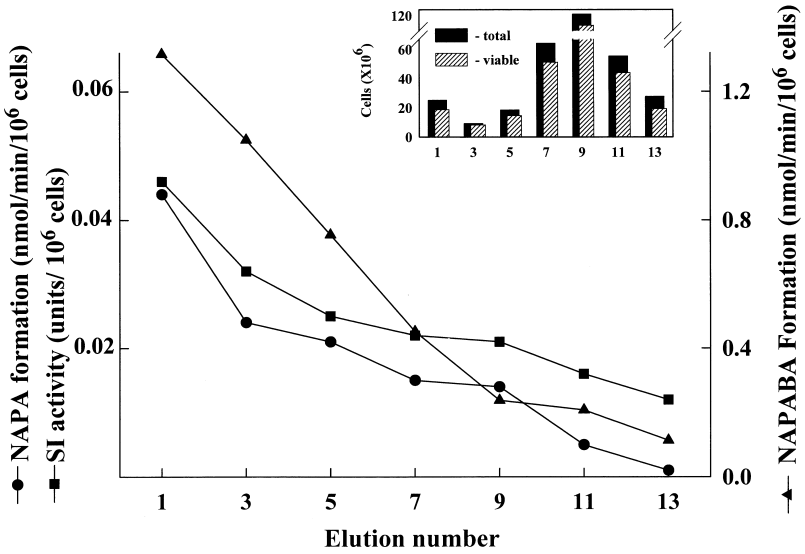

FIG. 1. Enterocyte NAT and SI activities from eluted cell fractions from a representative rat. For NAT activities, each point represents the mean of three replicates. For SI activity, each point represents the average of duplicate measurements. The inserted bar graph shows the total number of cells eluted in each fraction and the viable cells eluted.

standard-operating-procedures for handling of hazardous materials were followed to ensure the safety of laboratory personnel.] As has been demonstrated by Dahlqvist and Nordstrom [21] and Weiser [18], initial cell fractions contained higher amounts of SI activity, with decreasing activity found with increased fraction number collected. SI activity was calculated according to Dahlqvist [21, 24].

Data Analysis

Mean (±SD) velocity was reported for each isolated fraction with RMANOVA used to evaluate the hypothesis of vertical heterogeneity. One-way Kruskal–Wallis analysis of variance on ranks was used to compare viability from each isolated fraction.

RESULTS AND DISCUSSION

Studies investigating NAT heterogeneity along the duodenal-colonic axis suggest that a similar level of NAT1 and NAT2 expression exists throughout the length of the intestinal tract in the F-344 rat [6]. This lack of longitudinal heterogeneity in NAT expression does not necessarily rule out the importance of local bioactivation of HAs by NAT in determining the predisposition of colorectal tissue to tumor formation. Cellular heterogeneity may exist for NAT along the crypt-villus axis of the small intestine or crypt-to-surface axis of the large intestine, which could explain the preferential toxicity in the colorectal region. For example, if a xenobiotic undergoes bioactivation at or near the base of the crypt region, it is possible that these rapidly proliferating cells may be subject to genotoxic insult. In contrast, if the xenobiotic undergoes bioactivation at the villus-tip and forms a stable intermediate that is subsequently extruded into the lumen, NAT activation in the small intestine may result in delivery of a bioactivated form to the colorectal region.

Vertical heterogeneity has been shown in the expression of CYP and several brush-border membrane enzymes, including SI. Evaluation of SI activity in isolated cell suspensions, prepared by the chelation/elution method, indicates that the villus-tip and mid-villus cell populations contain the highest SI activity, with a decreasing gradient with increased fractions collected [18, 21–23]. Therefore, we utilized SI activity to determine whether a successful villus, mid-villus, and crypt cell gradient had been achieved during the timed chelation/elution protocol. There were no significant differences in the percentage of viable cells isolated from each fraction, although fraction 1 had the highest (85 ± 10%) and fraction 13 had the lowest (75 ± 7.1%) percentage of viable cells. Identification of cellular phenotype based on morphological evaluation of cellular suspensions was consistent with villus enrichment in fractions 1–9, which show high SI activity, while crypt enrichment was suggested by the morphological change of cells in the later fractions collected and a decrease in SI activity (data not shown).

The results of a representative cell isolation for determination of SI, NAT1, and NAT2 activity are shown in Fig. 1. The inserted bar graph represents the total number of cells eluted in each fraction, along with the percentage of viable cells. Utilizing SI as a marker enzyme for villus enrichment, a gradient of 4- to 10-fold was achieved. Tables 2 and 3 present the NAT1 and NAT2 activities when normalized per 10^6 cells or per milligram of cytosolic protein, respectively. As shown in Table 2, NAPA and NAPABA formation also followed this gradient, with the highest levels in fractions 1, 3, and 5 and the lowest levels in the final fractions (RMANOVA followed by SNK post-hoc comparisons, $P < 0.05$ for fractions 1, 3, and 5

TABLE 2. NAT1 and NAT2 activities in isolated enterocyte cell suspensions from F-344 rat small intestine expressed per 10^6 cells

Elution No.	NAT1 activity (nmol NAPA/min/10^6 cells)	NAT2 activity (nmol NAPABA/min/10^6 cells)	Ratio of NAT2:NAT1
1	0.029 ± 0.012	1.102 ± 0.406	38.52
3	0.030 ± 0.011	1.190 ± 0.517	39.38
5	0.023 ± 0.012	0.832 ± 0.416	36.50
7	0.016 ± 0.002	0.554 ± 0.123	34.62
9	0.013 ± 0.004	0.403 ± 0.135	31.03
11	0.010 ± 0.003	0.328 ± 0.086	33.51
13	0.005 ± 0.002	0.200 ± 0.064	41.62

*Data are presented as means ± SD of 5 animals. Based on RMANOVA followed by SNK post-hoc comparisons, NAPA and NAPABA were significantly greater ($P < 0.05$) in fractions 1, 3, and 5 vs fractions 7, 9, 11, or 13.

versus fractions 7, 9, 11, or 13). It is important to recognize that, as indicated previously, the viability of cells did not differ significantly among fractions collected. Therefore, the change in NAT1 and NAT2 activities is a reflection of either decreased content and/or activity of these enzymes in the crypt region. Because enterocytes comprise >90% of the cell population of the jejunal region of the intestine [7–10], it is presumed that NAT1 and NAT2 activities are a reflection of these cells. No attempt was made, however, to elucidate the contribution of the goblet cells, enteroendocrine cells, or Paneth cells to NAT activity. Of particular interest is the preferential distribution of NAT activities noted in the fully differentiated enterocytes, and the significant reduction in activity in the base or crypt-enriched fractions. The results of the present study are similar to those observed with the CYPs, though different from those that have been reported for the GSTs [11–17]. As the ratio of NAT2:NAT1 activity did not differ significantly among elutions, it appears that NAT1 and NAT2 exhibit identical cellular distribution in the rat small intestine. However, when NAT1 or NAT2 activity was normalized per milligram of cytosolic protein, no significant differences existed between elution fractions. The discrepancy between activities based upon normalization per 10^6 cells versus milligram of cytosolic protein may reflect the soluble protein that is not derived from actual cell cytosol (BSA in Buffer B). However, this should have been the same in each of the isolated cellular fractions. It is possible that the fraction of total cytosolic protein represented by NAT1 or NAT2 decreases moving from the villus tip to the crypt, which would result in the observed difference when normalized per 10^6 cells, but no difference when normalized per milligram of protein.

Since the time frame in which intestinal cells were exposed to buffer at 37° increased with each elution fraction, the possibility that the differential activity may be due to thermo-instability of NAT must be considered. However, we have shown previously that there is a 4- to 5-fold difference between the thermal inactivation constants for NAT1 and NAT2 from the small intestine of the F-344 rat [6]. Thus, if thermal inactivation were the cause of the differential activity seen with the various elution fractions, the NAT2:NAT1 ratio should also change significantly as a function of elution fraction. As shown in Tables 2 and 3, this ratio did not differ significantly in villus-enriched compared with crypt-enriched fractions. Thus, it is unlikely that thermal degradation can account for the differences in activity observed in various elution fractions.

Recent reports by other investigators using *in situ* hybridization in Sprague–Dawley rats would indicate that NAT mRNA is distributed equally along the length of the crypt-villus axis in this strain [25]. Our preliminary studies that measured NAT1 and NAT2 activities in the Sprague–Dawley rat also supported these observations (data not shown), which is in contrast to what we observed in the F-344 rat (Table 2). Further work is needed to substantiate these findings. However, if substantiated, comparison of the

TABLE 3. NAT1 and NAT2 activities in isolated enterocyte cell suspensions from F-344 rat small intestine expressed per milligram of cytosolic protein*

Elution No.	NAT1 activity (nmol NAPA/min/mg protein)	NAT2 activity (nmol NAPABA/min/mg protein)	Ratio of NAT2:NAT1
1	0.094 ± 0.039	3.63 ± 1.18	38.59
3	0.074 ± 0.029	2.99 ± 1.37	40.63
5	0.100 ± 0.064	3.55 ± 1.80	35.56
7	0.100 ± 0.023	3.50 ± 0.89	34.56
9	0.106 ± 0.049	3.27 ± 1.90	30.89
11	0.068 ± 0.030	2.21 ± 0.75	32.67
13	0.042 ± 0.035	1.76 ± 1.25	42.05

*Data are presented as means ± SD of 5 animals.

susceptibility of these two strains to regiospecific tumor formation after administration of HAs would provide a good test of the role of this heterogeneous expression in determining susceptibility to carcinogens.

Studies to determine the cellular localization of NAT within the crypt-villus axis suggest that both NAT1 and NAT2 are heterogeneously expressed in the crypt to villus-tip cell populations. This may result in delivery of bioactivated HA to the lower regions of the intestines, as the villus-tip cells are extruded into the intestinal lumen and enter the fecal stream. This phenomenon may contribute to the predisposition of the colorectal region to the development of tumors after HA ingestion.

This work was supported, in part, by Public Health Service Grant GM45203 to Dr. Svensson.

References

1. Kaminsky LS and Fasco MJ, Small intestinal cytochromes P450. *Crit Rev Toxicol* **21:** 407–422, 1992.
2. Ilett KF, Tee LBG, Reeves PT and Minchen RF, Metabolism of drugs and other xenobiotics in the gut lumen and wall. *Pharmacol Ther* **46:** 67–93, 1990.
3. Gillette JR, A perspective on the role of chemically reactive metabolites of foreign compounds in toxicity—I. Correlation of changes in covalent binding of reactive metabolites with changes in the incidence and severity of toxicity. *Biochem Pharmacol* **23:** 2785–2794, 1974.
4. Miller EC and Miller JA, Searches for ultimate chemical carcinogens and their reactions with cellular macromolecules. *Cancer* **47:** 2327–2345, 1981.
5. Ito N, Hasegawa R, Sano M, Tamano S, Esumi H, Takayama S and Sugimura T, A new colon and mammary carcinogen in cooked food, 2-amino-1-methyl-6-phenylimidazo[4,5-*b*]pyridine (PhIP). *Carcinogenesis* **12:** 1503–1506, 1991.
6. Ware JA and Svensson CK, Longitudinal distribution of arylamine *N*-acetyltransferases in the intestine of the hamster, mouse, and rat. Evidence for multiplicity of *N*-acetyltransferases in the intestine. *Biochem Pharmacol* **52:** 1613–1620, 1996.
7. Cheng H and Leblond CP, Origin, differentiation and renewal of the four main epithelial cell types in the mouse small intestine. I. Columnar cell. *Am J Anat* **141:** 461–479, 1974.
8. Cheng H, Origin, differentiation and renewal of the four main epithelial cell types in the mouse small intestine. II. Mucous cells. *Am J Anat* **141:** 481–502, 1974.
9. Cheng H and Leblond CP, Origin, differentiation and renewal of the four main epithelial cell types in the mouse small intestine. III. Entero-endocrine cells. *Am J Anat* **141:** 503–520, 1974.
10. Cheng H, Origin, differentiation and renewal of the four main epithelial cell types in the mouse small intestine. IV. Paneth cells. *Am J Anat* **141:** 521–536, 1974.
11. Bonkovsky HL, Hauri HP, Marti U, Gasser R and Meyer UA, Cytochrome P450 of small intestinal epithelial cells. Immunochemical characterization of the increase in cytochrome P450 caused by phenobarbital. *Gastroenterology* **88:** 458–467, 1985.
12. Watkins PB, Wrighton SA, Schuetz EG, Molowa DT and Guzelian PS, Identification of glucocorticoid-inducible cytochrome P-450 in the intestinal mucosa of rats and man. *J Clin Invest* **80:** 1029–1036, 1987.
13. Traber PG, Chianale J, Florence R, Kim K, Wojcik E and Gumucio JJ, Expression of cytochromes P450b and P450e genes in small intestinal mucosa of rats following treatment with phenobarbital, polyhalogenated biphenyls, and organochlorine pesticides. *J Biol Chem* **263:** 9449–9455, 1988.
14. Traber PG, Wang W and Yu L, Differential regulation of cytochrome P-450 genes along rat intestinal crypt-villus axis. *Am J Physiol* **263:** G215–G223, 1992.
15. Fasco MJ, Silkworth JB, Dunbar DA and Kaminsky LS, Rat small intestinal cytochromes P450 probed by warfarin metabolism. *Mol Pharmacol* **43:** 226–233, 1993.
16. Zhang QY, Wikoff J, Dunbar DA, Fasco MJ and Kaminisky LS, Regulation of cytochrome P4501A1 expression in rat small intestine. *Drug Metab Dispos* **25:** 21–26, 1997.
17. Dubey RK and Singh J, Localization and characterization of drug-metabolizing enzymes along the villus-crypt surface of the rat small intestine—II. Conjugases. *Biochem Pharmacol* **37:** 177–184, 1988.
18. Weiser MM, Intestinal epithelial cell surface membrane glycoprotein synthesis. I. An indicator of cellular differentiation. *J Biol Chem* **248:** 2536–2541, 1973.
19. Svensson CK and Tomilo M, Effect of H_2-receptor antagonists on rat liver cytosolic acetyl CoA:arylamine *N*-acetyltransferase activity. *Drug Metab Dispos* **20:** 74–78, 1992.
20. Drobitch RK, Tomilo M and Svensson CK, Immunomodulation and drug acetylation: Influence of the immunomodulator tilorone on hepatic, renal and blood *N*-acetyltransferase activity and on hepatic cytosolic acetyl coenzyme A content. *Biochem Pharmacol* **43:** 1643–1648, 1992.
21. Dahlqvist A and Nordstrom C, The distribution of disaccharisdase activities in the villi and crypts of the small-intestinal mucosa. *Biochim Biophys Acta* **113:** 624–626, 1966.
22. Traber PG, Yu L, Wu GD and Judge TA, Sucrase-isomaltase gene expression along crypt-villus axis of human small intestine is regulated at level of mRNA abundance. *Am J Physiol* **262:** G123–G130, 1992.
23. Chandrasena G, Sunitha I, Lau C, Nanthakumar NN and Henning SJ, Expression of sucrase-isomaltase mRNA along the villus-crypt axis in the rat small intestine. *Cell Mol Biol* **38:** 243–254, 1992.
24. Dahlqvist A, Method of assay of intestinal disaccharidases. *Anal Biochem* **7:** 18–25, 1964.
25. Debiec-Rychter M, Land S and King CM, Histological localization of messenger RNAs for rat acetyltransferases that acetylate serotonin and genotoxic arylamines. *Cancer Res* **56:** 1517–1525, 1996.